

New Accurate Approximation for Average Error Probability Under $\kappa - \mu$ Shadowed Fading Channel

Yassine Mouchtak, Faissal El Bouanani

ENSIAS, Mohammed V University in Rabat

e-mails: {yassine.mouchtak,f.elbouanani}@um5s.net.ma

Corresponding author: Faissal El Bouanani.

Abstract

This paper proposes new accurate approximations for average error probability (AEP) of a communication system employing either M -phase-shift keying (PSK) or differential quaternary PSK with Gray coding (GC-DQPSK) modulation schemes over $\kappa - \mu$ shadowed fading channel. Firstly, new accurate approximations of error probability (EP) of both modulation schemes are derived over additive white Gaussian noise (AWGN) channel. Leveraging the trapezoidal integral method, a tight approximate expression of symbol error probability for M -PSK modulation is presented, while new upper and lower bounds for Marcum Q -function of the first order (MQF), and subsequently those for bit error probability (BER) under DQPSK scheme, are proposed. Next, these bounds are linearly combined to propose a highly refined and accurate BER's approximation. The key idea manifested in the decrease property of modified Bessel function I_v , strongly related to MQF, with its argument v . Finally, these approximations are used to tackle AEP's approximation under $\kappa - \mu$ shadowed fading. Numerical results show the accuracy of the presented approximations compared to the exact ones.

Index Terms

Bit error rate, bounds refinement, DQPSK modulation, $\kappa - \mu$ shadowed fading, M -PSK modulation, Marcum Q -function, symbol error rate, upper bound.

I. INTRODUCTION

Wireless technologies are becoming part of our daily lives and their utilization increase rapidly due to many advantages such as cost-effectiveness, global coverage and flexibility.

Nevertheless, these technologies are infected by many phenomena including shadowing which is relatively slow and gives rise to long-term signal variations and multipath fading which is due to constructive and destructive interferences as a result of delayed, diffracted, reflected, and scattered signal components [1]. A great number of communication channels' models have been proposed in the literature to describe either the fading or the joint shadowing/fading phenomena [2]-[5]. Recently, the $\kappa - \mu$ shadowed fading proposed in [6], has attracted a lot of interest due to its versatility and wide applicability in practical scenarios. For instance, it was used for characterizing signal reception in device-to-device communications, body-to-body communications, underwater acoustic, fifth-generation (5G) communications, and satellite communication systems [7]-[11]. In addition, it was shown that numerous statistical models can be derived from the $\kappa - \mu$ shadowed one by setting the parameters to some specific real positive values [12]. Particularly, when the parameters μ and m are integer, such a model is equivalent to what's referred to as composite fading, namely, mixture Gamma distribution [13].

The average error probability (AEP) is a fundamental performance evaluation tool in digital communications, quantifying the reliability of an instantaneous received signal. Furthermore, dealing with the average EP (AEP) is quite practical in most applications as it states the average performance irrespective of time. Nonetheless, evaluating AEP in closed form remains a big challenge for numerous communication systems because of the complexity of either the end-to-end fading model or the employed modulation technique. Essentially, depending on the employed modulation scheme, EP is provided in either complicated integral form [1] or first-order Marcum Q -function (MQF) and the zeroth-order modified Bessel function (MBF) of the first kind [14] for various M -ary and differential quadrature phase-shift keying (DQPSK) modulation schemes, respectively. That integral form can be reexpressed also in terms Gaussian Q -function (GQF), which is not known in closed form. By its turn, the MQF integral-form involves the MBF with exponential term [1], that can be rewritten appropriately as an upper incomplete upper Fox's H-function (UIFH), or equivalently, an infinite summation of the product of upper incomplete Gamma functions [15]. Thus, obtaining AEP requires the averaging of a UIFH over a generalized fading distribution, which is not evident particularly for fading model with probability density function (PDF) involving the product of exponential and Fox's H- functions (e.g. $\kappa - \mu$ shadowed model). Obviously, deriving accurate bounds or approximations for the AEP is strongly depending on the EP's ones. To this end, several EP's bounds and approximations for the EP are proposed in the literature, for instance, in [16]-[19], numerous bounds for the symbol error

probability (SEP) in the case of M -ary PSK modulation are derived in terms of GQF and its powers. Such a function is itself mathematically intractable when involved in complicated integrals resulting from generalized fading distributions. To remedy this problem, several various works deal with simple, and accurate approximations or bounds for GQF when applied to inspect the performance of a communication system experiencing to a particular bivariate-Fox's H-fading model [20], [21]. In contrast, evaluating the performance of GC-DQPSK modulation requires simple bounds or approximate expressions for MQF due to its complicated closed-form and intractability when involved in the computation of AEP [22]-[25]. In [26] and [27], bounds for EP are investigated, while in [28], new lower and upper bounds for EP were proposed, based on which a novel approximation was derived. Despite the good accuracy of the latter's bounds and/or approximation for both MPSK and GC-DQPSK, they remain useless for AEP computation because of their forms' complications.

A. Motivation

The performance of wireless communication systems, with perfect channel state information (CSI) knowledge at the receiver, is widely examined by the scientific community. However, imperfect estimation of channel coefficients is dealt with various practical scenarios, leading to a significant degradation of the system performance. To overcome this limitation, differential modulation (DM) can be considered as an alternative solution particularly for low-power wireless systems, such as wireless sensor networks and relay networks [29]. The main advantage of this scheme is its simplicity of detection due to the unnecessary channel coefficients estimation and tracking, leading to significant reduction in the receiver computational complexity [30], [31]. However, this comes at a cost of higher error rate or lower spectral efficiency. As a result, selecting the most suitable modulation scheme depends on the considered application and both coherent and non-coherent detections. To this end, this paper is devoted to analyzing the performance of two modulation schemes, namely M -PSK and DQPSK over $\kappa - \mu$ shadowed fading channel.

B. Contribution

Capitalizing on the above, we aim at this work to propose accurate approximations for AEP under $\kappa - \mu$ shadowed fading and aforementioned modulation schemes. Specifically, utilizing the trapezoidal integral method, the EP integral form for various M -ary modulation schemes is

tightly approximated particularly for M -PSK scheme, while for DQPSK technique, we start by deriving simple lower and upper bounds for EP by bounding MQF, to be used jointly in finding AEP for generalized fading models.

Pointedly, our main key contributions can be summarized as follows

- We propose a new exponential type approximation for the EP's first form applied to M -PSK modulation by using the trapezoidal technique integral. To the best of the authors' knowledge, such accurate EP's approximation outperforms those presented in the literature,
- We derive new upper and lower bounds of EP in the case of DQPSK modulation based on which an accurate approximation of SEP is proposed,
- We provide, relying on the two proposed EP's approximations, a tight approximate expression for AEP over $\kappa - \mu$ shadowed fading channel,
- We provide the asymptotic analysis for both forms of AEP and we demonstrate that the diversity order over $\kappa - \mu$ shadowed fading channel remains constant.

Motivated by this introduction, the rest of this paper can be structured as follows. Methods and analysis used are described briefly in Section II. In section III, a new approximation for the first EP form (i.e., M -ary modulation) is presented for M -PSK while, new lower and upper bound of EP in the case of DQPSK are derived, based on which an accurate approximation for the EP is deduced. In Section IV, the expression of AEP under $\kappa - \mu$ shadowed fading for both modulation schemes is evaluated. In section V, the respective results are illustrated and verified by comparison with the exact ones using simulation computing. Section VI summarizes the main conclusions.

II. METHODS

The present work deal with the performance analysis of a wireless communication system subject to $\kappa - \mu$ shadowed fading. To this end, various methods are applied to derive new accurate approximate expressions for the error probability. Pointedly, the Trapezoedial integral technique is utilized to propose a simple approximation for the SEP in the case of M -PSK modulation, while bounding technique is used to derive upper and lower bounds for the bit error probability (BEP) in the case of GC-DQPSK modulation. Furthermore, by using Matlab curve fitting application, a refinement is applied on these two new bounds to obtain a novel accurate approximation for the BEP of this latter modulation scheme. Next, the approximations of the EP

are used to derive tight approximation for the AEP under the considered fading model. Lastly, the accuracy of the derived AEP's approximation is validated using Monte carlo simulation.

III. BOUNDS ON THE SEP

In this section, we propose new approximate expressions for the two potential different forms of EP, namely (i) complicated integral form, and (ii) MQF form, applied to M -PSK and DQPSK modulations with Gray coding, respectively.

A. EP with integral form

Proposition 1. *The SEP for M -PSK modulation can be tightly approximated by*

$$\tilde{\mathcal{H}}_1(\gamma) \simeq \sum_{l=1}^7 \mathcal{A}_l \exp(-\mathcal{B}_l \gamma), \quad (1)$$

while \mathcal{A}_l and \mathcal{B}_l are given in Table I.

TABLE I
THE COEFFICIENTS \mathcal{A}_l AND \mathcal{B}_l .

l	1	2	3	4	5	6	7
\mathcal{A}_l	$\frac{7M-8}{48M}$	$\frac{1}{8}$	$\frac{1}{8}$	$\frac{1}{8}$	$\frac{M-2}{12M}$	$\frac{M-2}{6M}$	$\frac{M-2}{6M}$
\mathcal{B}_l	ϱ	2ϱ	$\frac{20\varrho}{3}$	$\frac{20\varrho}{17}$	$\frac{\varrho}{\cos^2(\frac{M-2}{2M}\pi)}$	$\frac{\varrho}{\cos^2(\frac{M-2}{6M}\pi)}$	$\frac{\varrho}{\cos^2(\frac{M-2}{3M}\pi)}$

Proof. The SEP for M -PSK modulation is given as [1, Eq. (8.22)]

$$\mathcal{H}_1(\gamma) = \frac{1}{\pi} \int_0^{\frac{M-1}{M}\pi} \exp\left(-\frac{\varrho\gamma}{\sin^2(\theta)}\right) d\theta, \quad (2)$$

with

$$\varrho = \log_2(M) \sin^2\left(\frac{\pi}{M}\right), \quad (3)$$

and γ denotes the signal-to-noise (SNR) ratio per bit.

Subsequently, (2) can be written as

$$\mathcal{H}_1(\gamma) = Q\left(\sqrt{2\varrho\gamma}\right) + \underbrace{\frac{1}{\pi} \int_0^{\frac{M-2}{2M}\pi} \exp\left(-\frac{\varrho\gamma}{\cos^2(t)}\right) dt}_{\mathcal{I}} \quad (4)$$

where $Q(\cdot)$ denotes the Gaussian Q -Function [1, Eq. (4.1)].

The integral \mathcal{I} can be approximated using numerical integration rules. The trapezoidal rule for definite integration of an arbitrary function between $[x_0, x_0 + n\phi]$ is given by

$$\int_{x_0}^{x_0+n\phi} f(t) dt = \frac{\phi}{2} \left[g_0 + g_n + 2 \sum_{i=1}^{n-1} g_i \right],$$

where $g_i = f(x_0 + i\phi)$ for $i = 0..n$, n refers to the number of sub-intervals equally spaced trapeziums, and ϕ defines the spacing. Note that greater n the higher the accuracy's approximation and the computational complexity as well.

By setting $n = 3$ and $f(t) = \exp[-\varrho\gamma/\cos^2(t)]$, \mathcal{I} can be approximated as

$$\begin{aligned} \mathcal{I} \simeq & \frac{M-2}{12M} \left[\begin{array}{c} \exp(-\varrho\gamma) \\ + \exp\left(-\frac{\varrho\gamma}{\cos^2(\frac{M-2}{2M}\pi)}\right) \end{array} \right] \\ & + \frac{M-2}{6M} \left[\begin{array}{c} \exp\left(-\frac{\varrho\gamma}{\cos^2(\frac{M-2}{6M}\pi)}\right) \\ + \exp\left(-\frac{\varrho\gamma}{\cos^2(\frac{M-2}{3M}\pi)}\right) \end{array} \right]. \end{aligned} \quad (5)$$

By plugging [32, Eq. (8b)] and (5) in (4), (13) is attained. ■

Table II confirms the accuracy of the proposed approximation. Interestingly, one can ascertain that this tightness can be further improved by increasing n , i.e., by increasing the number of terms in the approximation.

B. EP with MQF form

The bit error probability (BEP) for DQPSK modulation with Gray coding is given by [14]

$$\mathcal{H}_2(\gamma) = Q_1(a\sqrt{\gamma}, b\sqrt{\gamma}) - \frac{1}{2}I_0(\sqrt{2}\gamma) \exp(-2\gamma), \quad (6)$$

with γ denotes the SNR per bit, $a = \sqrt{2(1 - \sqrt{0.5})}$, $b = \sqrt{2(1 + \sqrt{0.5})}$, $I_v(\cdot)$ is the v -th order modified Bessel function of the first kind [15, Eq. (8.431)], and $Q_1(\cdot, \cdot)$ represents the first-order MQF defined as [1, Eq. (4.34)]

$$Q_1(\alpha, \beta) = \int_{\beta}^{\infty} t \exp\left(-\frac{t^2 + \alpha^2}{2}\right) I_0(\alpha t) dt. \quad (7)$$

TABLE II
COMPARISON BETWEEN THE EXACT AND APPROXIMATE SEP FOR M -PSK MODULATION.

$M = 4$							
γ	1	2	3	4	5	6	7
SEP							
$\mathcal{H}_1(\gamma)$, Eq. (2)	1.508×10^{-1}	4.494×10^{-2}	1.425×10^{-2}	4.672×10^{-3}	1.565×10^{-3}	5.319×10^{-4}	1.828×10^{-4}
$\tilde{\mathcal{H}}_1(\gamma)$, Eq. (1)	1.501×10^{-1}	4.460×10^{-2}	1.414×10^{-2}	4.642×10^{-3}	1.556×10^{-3}	5.289×10^{-4}	1.816×10^{-4}
$M = 8$							
γ	2	4	6	8	10	14	16
SEP							
$\mathcal{H}_1(\gamma)$, Eq. (2)	1.849×10^{-1}	6.083×10^{-2}	2.167×10^{-2}	8.018×10^{-3}	3.034×10^{-3}	4.526×10^{-4}	1.772×10^{-4}
$\tilde{\mathcal{H}}_1(\gamma)$, Eq. (1)	1.847×10^{-1}	6.077×10^{-2}	2.156×10^{-2}	7.976×10^{-3}	3.022×10^{-3}	4.504×10^{-4}	1.760×10^{-4}
$M = 16$							
γ	5	10	20	30	35	40	45
SEP							
$\mathcal{H}_1(\gamma)$, Eq. (2)	2.173×10^{-1}	8.100×10^{-2}	1.360×10^{-2}	2.508×10^{-3}	1.096×10^{-3}	4.832×10^{-4}	2.143×10^{-4}
$\tilde{\mathcal{H}}_1(\gamma)$, Eq. (1)	2.177×10^{-1}	8.072×10^{-2}	1.358×10^{-2}	2.500×10^{-3}	1.091×10^{-3}	4.794×10^{-4}	2.122×10^{-4}

1) *New lower bound for BEP:*

Proposition 2. *The BEP for DQPSK modulation with Gray coding can be lower bounded as*

$$\mathcal{H}_2(\gamma) \geq \mathcal{L}(\gamma), \quad (8)$$

with

$$\mathcal{L}(\gamma) \triangleq \delta \mathcal{K}(a, b, \gamma) - \frac{1}{2} I_0(\sqrt{2}\gamma) \exp(-2\gamma), \quad (9)$$

$$\mathcal{K}(a, b, \gamma) = Q((b-a)\sqrt{\gamma}) - Q((b+a)\sqrt{\gamma}), \quad (10)$$

and $Q(\cdot)$ denotes the Gaussian Q -function [1, Eq. (4.1)], and $\delta = \sqrt{\frac{b}{a}}$.

Proof. As I_v is a decreasing function with respect to the index v [33], yields

$$Q_1(a\sqrt{\gamma}, b\sqrt{\gamma}) \geq \mathcal{J}, \quad (11)$$

with

$$\mathcal{J} \triangleq \int_{b\sqrt{\gamma}}^{\infty} t \exp\left(-\frac{t^2 + a^2\gamma}{2}\right) I_{\frac{1}{2}}(a\sqrt{\gamma}t) dt. \quad (12)$$

Now applying [15, Eq. (8.431.4)] for $v = \frac{1}{2}$, one can ascertain

$$I_{\frac{1}{2}}(a\sqrt{\gamma}t) = \frac{2 \sinh(a\sqrt{\gamma}t)}{\sqrt{2\pi a\sqrt{\gamma}t}}, \quad (13)$$

where $\sinh(\cdot)$ accounts for the hyperbolic sine function.

By plugging (13) into (12) along with the following identity

$$\sinh(a\sqrt{\gamma}t) = \frac{\exp(a\sqrt{\gamma}t) - \exp(-a\sqrt{\gamma}t)}{2}, \quad (14)$$

one can obtain

$$\mathcal{J} \geq \frac{1}{\sqrt{2\pi a}} \int_{b\sqrt{\gamma}}^{\infty} \sqrt{\frac{t}{\sqrt{\gamma}}} \left[\begin{array}{c} \exp\left(-\frac{(t-a\sqrt{\gamma})^2}{2}\right) \\ - \exp\left(-\frac{(t+a\sqrt{\gamma})^2}{2}\right) \end{array} \right] dt. \quad (15)$$

Finally, as $t \geq b\sqrt{\gamma}$, yields

$$\begin{aligned} \mathcal{J} &\geq \frac{\delta}{\sqrt{2\pi}} \left[\begin{array}{c} \int_{b\sqrt{\gamma}}^{\infty} \exp\left(-\frac{(t-a\sqrt{\gamma})^2}{2}\right) dt \\ - \int_{b\sqrt{\gamma}}^{\infty} \exp\left(-\frac{(t+a\sqrt{\gamma})^2}{2}\right) dt \end{array} \right] \\ &= \frac{\delta}{\sqrt{2\pi}} \mathcal{K}(a, b, \gamma), \end{aligned} \quad (16)$$

which concludes the proof. ■

2) *New upper bound for BEP:*

Proposition 3. For $\gamma \geq 0$, holds

$$\mathcal{H}_2(\gamma) \leq \mathcal{U}(\gamma),$$

with

$$\mathcal{U}(\gamma) \triangleq \frac{1}{\delta} \mathcal{K}(a, b, \gamma) + \frac{1}{2} I_0(\sqrt{2\gamma}) \exp(-2\gamma). \quad (17)$$

Proof. Relying on (7) and using integration by part by considering $u'(t) = t \exp\left(-\frac{t^2}{2}\right)$ and $w = I_0(\sqrt{a\gamma}t)$, one can see

$$Q_1(a\sqrt{\gamma}, b\sqrt{\gamma}) = \mathcal{T} + I_0(\sqrt{2\gamma}) \exp(-2\gamma),$$

with

$$\mathcal{T} = \int_{b\sqrt{\gamma}}^{\infty} a\sqrt{\gamma} \exp\left(-\frac{t^2 + a^2\gamma}{2}\right) I_1(a\sqrt{\gamma}t) dt. \quad (18)$$

Again, by incorporating the inequality $I_1(t) \leq I_{\frac{1}{2}}(t)$ [33], alongside with (13) and (14) into (18), we get

$$\mathcal{T} \leq \sqrt{\frac{a\sqrt{\gamma}}{2\pi}} \int_{b\sqrt{\gamma}}^{\infty} \frac{1}{\sqrt{t}} \left[\begin{array}{c} \exp\left(-\frac{(t-a\sqrt{\gamma})^2}{2}\right) \\ -\exp\left(-\frac{(t+a\sqrt{\gamma})^2}{2}\right) \end{array} \right] dt. \quad (19)$$

Moreover, as $t \geq b\sqrt{\gamma}$ in the aforementioned integrand, one can check

$$\mathcal{T} \leq \frac{1}{\delta} \mathcal{K}(a, b, \gamma). \quad (20)$$

Therefore (17) can be inferred from (20) jointly with (10); this completes the proof. \blacksquare

3) *Approximate BEP for DQPSK*: In this part, a tight approximate expression for the BEP under DQPSK scheme is derived based on the two bounds presented above. In a similar manner to the approach followed in [28], the new proposed approximation is a linear combination of the two aforementioned bounds for $\mathcal{H}_2(\gamma)$, namely

$$\tilde{\mathcal{H}}_2(\gamma) = \tilde{\chi}(\gamma)\mathcal{U}(\gamma) + (1 - \tilde{\chi}(\gamma))\mathcal{L}(\gamma). \quad (21)$$

Proposition 4. *The function $\chi(\gamma)$ can be chosen as*

$$\tilde{\chi}(\gamma) = \mathcal{C}_0 \exp(-\mathcal{D}_0\gamma) + \mathcal{C}_1 \exp(-\mathcal{D}_1\gamma), \quad (22)$$

where \mathcal{C}_i and \mathcal{D}_i are the best-fit parameters, depending on the SNR interval, summarized in Table III.

TABLE III
OPTIMUM VALUES OF FITTING PARAMETERS FOR DIFFERENT SNR RANGES.

C_i, \mathcal{D}_i	\mathcal{C}_0	\mathcal{D}_0	\mathcal{C}_1	\mathcal{D}_1
SNR range				
$\gamma < 1$	0.1786	2.903	0.7564	0.1307
$1 \leq \gamma < 8$	0.3798	1.895	0.6183	7.93×10^{-4}
$\gamma > 8$	0.005206	0.2764	0.6146	5.593×10^{-5}

Proof. First, note that the following function

$$\chi(\gamma) = \frac{\mathcal{H}(\gamma) - \mathcal{L}(\gamma)}{\mathcal{U}(\gamma) - \mathcal{L}(\gamma)}, \quad (23)$$

satisfies the identity

$$\mathcal{H}_2(\gamma) = \chi(\gamma)\mathcal{U}(\gamma) + (1 - \chi(\gamma))\mathcal{L}(\gamma). \quad (24)$$

That is, it is sufficient to look for a tight approximation for (23) so as to approximate $\mathcal{H}_2(\gamma)$.

By plotting $\chi(\gamma)$ as shown in Fig. 1, one can clearly notice its exponential behavior. It follows that its approximate expression can be written in the form (22). Furthermore, the optimized coefficients \mathcal{C}_i and \mathcal{D}_i outlined in Table III, for various SNR intervals can be straight forward obtained using a curve fitting tool (e.g., Matlab Curve Fitting app); this ends the proof. ■

Remark 1. *It is worthwhile that the first-order MQF can be approximated, relying on (6) and (21), by*

$$\begin{aligned}\tilde{Q}_1(a\sqrt{\gamma}, b\sqrt{\gamma}) &= \tilde{\mathcal{H}}_0(\gamma) + \frac{1}{2}I_0(\sqrt{2}\gamma) \exp(-2\gamma) \\ &= \mathcal{K}(a, b, \gamma) (\eta\tilde{\chi}(\gamma) + \delta) \\ &\quad + I_0(\sqrt{2}\gamma) \exp(-2\gamma) \tilde{\chi}(\gamma).\end{aligned}\quad (25)$$

Both exact and approximate functions $\chi(\gamma)$ and $\tilde{\chi}(\gamma)$ are plotted in Fig. 1. One can observe that there exists a strong matching between the two curves over the entire range of γ .

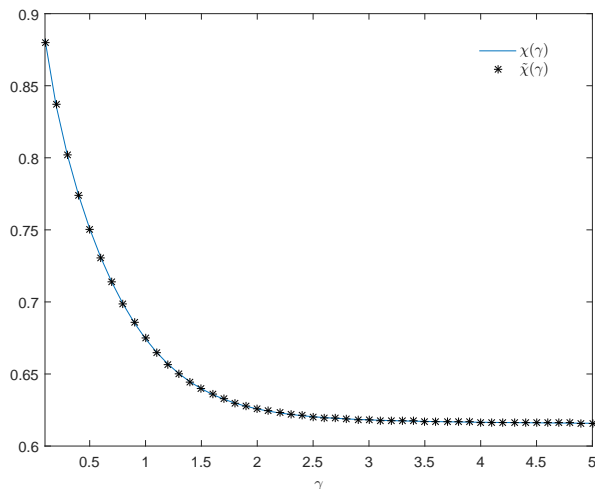


Fig. 1. Comparison between $\chi(\gamma)$ and $\tilde{\chi}(\gamma)$.

Table IV summarizes the accuracy of the proposed approximation compared with the best ones proposed in the literature, namely $\{\tilde{\mathcal{H}}_i(\gamma)\}_{i=3..5}$ labeled $\{BER_{i+2}\}_{i=3..5}$ in [28], respectively. Besides, the relative error corresponding to the aforementioned approximations, namely

$$\varepsilon_i = \frac{|\tilde{\mathcal{H}}_i(\gamma) - \mathcal{H}_2(\gamma)|}{\mathcal{H}_2(\gamma)}, i = 2..5.,$$

TABLE IV
COMPARISON BETWEEN THE EXACT AND APPROXIMATE BEP

γ	Eq. (6)	$\tilde{H}_2(\gamma)$, Eq. (21)	$\tilde{H}_3(\gamma)$, [28]	$\tilde{H}_4(\gamma)$, [28]	$\tilde{H}_5(\gamma)$, [28]
0.5	2.6929×10^{-1}	2.6918×10^{-1}	2.7792×10^{-1}	2.6921×10^{-1}	2.6911×10^{-1}
1	1.6391×10^{-1}	1.6395×10^{-1}	1.6383×10^{-1}	1.6383×10^{-1}	1.6568×10^{-1}
1.5	1.0646×10^{-1}	1.0645×10^{-1}	1.0667×10^{-1}	1.0655×10^{-1}	1.0667×10^{-1}
2	7.1611×10^{-2}	7.1614×10^{-2}	7.1685×10^{-2}	7.1625×10^{-2}	7.1885×10^{-2}
2.5	4.9177×10^{-2}	4.9178×10^{-2}	4.9190×10^{-2}	4.9174×10^{-2}	4.9481×10^{-2}
3	3.4227×10^{-2}	3.4226×10^{-2}	3.4228×10^{-2}	3.4226×10^{-2}	3.4482×10^{-2}
4	1.7013×10^{-2}	1.7013×10^{-2}	1.7015×10^{-2}	1.7018×10^{-2}	1.7144×10^{-2}
5	8.6484×10^{-3}	8.6485×10^{-3}	8.6501×10^{-3}	8.6501×10^{-3}	8.7059×10^{-3}
6	4.4613×10^{-3}	4.4613×10^{-3}	4.4624×10^{-3}	4.4617×10^{-3}	4.4859×10^{-3}
7	2.3256×10^{-3}	2.3256×10^{-3}	2.3263×10^{-3}	2.3257×10^{-3}	2.3363×10^{-3}
8	1.2219×10^{-3}	1.2219×10^{-3}	1.2222×10^{-3}	1.2219×10^{-3}	1.2266×10^{-3}
9	6.4596×10^{-4}	6.4597×10^{-4}	6.4613×10^{-4}	6.4597×10^{-4}	6.4594×10^{-4}
10	3.4318×10^{-4}	3.4319×10^{-4}	3.4327×10^{-4}	3.4319×10^{-4}	3.4318×10^{-4}
11	1.8307×10^{-4}	1.8307×10^{-4}	1.8311×10^{-4}	1.8307×10^{-4}	1.8307×10^{-4}
12	9.7990×10^{-5}	9.7990×10^{-5}	9.8011×10^{-5}	9.7990×10^{-5}	9.7990×10^{-5}

is depicted in Fig. III-B3. Obviously, the relative error corresponding to the proposed approximation outperforms those in [28], except for a short interval, i.e., [11.7, 12.45] where $\mathcal{H}_2(\gamma)$ is negligible, as outlined in Table II, compared to its values getting for small SNR.

Remark 2. *It can be seen clearly that the proposed approximation outperforms the concurrent ones. Moreover, one can check that the three expressions $\{\tilde{\mathcal{H}}_i(\gamma)\}_{i=3..5}$ are tough, which rend them useless in numerous applications such as the average bit error probability (ABEP) computation under a complicated fading model. Contrarily, the expression of $\tilde{\mathcal{H}}_2(\gamma)$ is quite simple, making it more appropriate for various fields.*

IV. AEP ANALYSIS

As mentioned above, the proposed approximate EP is used to derive an approximate AEP when communicating over $\kappa - \mu$ shadowed fading.

The PDF of instantaneous SNR γ under the $\kappa - \mu$ shadowed fading model can be written as [12, Eq. 4]

$$f_\gamma(\gamma) = \frac{\lambda}{\Gamma(\mu)} \gamma^{\mu-1} e^{-\nu\gamma} {}_1F_1(m; \mu; \omega\gamma), \quad (26)$$

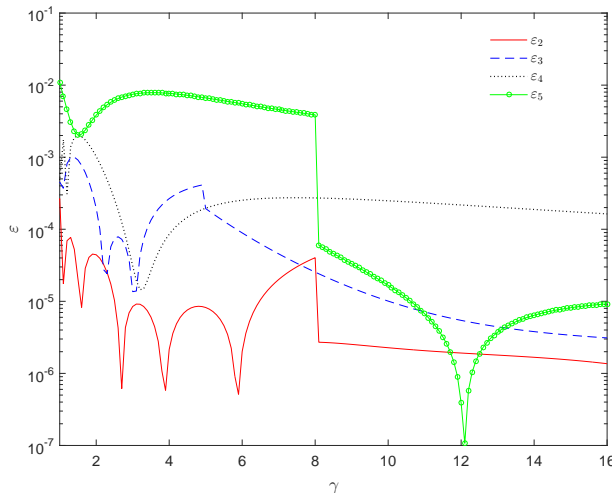


Fig. 2. Comparison of the relative errors.

with

$$\lambda = \frac{\mu^\mu m^m (1 + \kappa)^\mu}{\bar{\gamma}^\mu (\mu\kappa + m)^m}, \quad \nu = \frac{\mu(1 + \kappa)}{\bar{\gamma}}, \quad \omega = \frac{\mu^2 \kappa (1 + \kappa)}{\bar{\gamma}(\mu\kappa + m)}, \quad (27)$$

where $\bar{\gamma}$ is the average SNR, κ indicates the power ratio between the dominant waves, μ refers to the scattered components, while m accounts for the shape parameter. Further, ${}_1F_1(\cdot; \cdot; \cdot)$ and $\Gamma(\cdot)$ denote the Kummer confluent hypergeometric and Euler Gamma functions, respectively.

The AEP approximation for both M -PSK and DQPSK schemes can be straightforwardly evaluated as

$$P_e = \int_0^\infty f(\gamma) \mathcal{H}_i(\gamma) d\gamma, \quad (28)$$

by setting $i = 1$ and $i = 2$, respectively.

Remark 3. P_e accounts for the average symbol error probability (ASEP) for M -PSK modulation, while it refers to the ABEP for DQPSK modulation with Gray coding.

Proposition 5. In the case of M -PSK modulation, the ASEP over $\kappa - \mu$ shadowed fading model can be approximated as

$$P_e \simeq \lambda \sum_{l=1}^7 \mathcal{A}_l (\nu + \mathcal{B}_l)^{-\mu} \left(1 - \frac{\omega}{\nu + \mathcal{B}_l}\right)^{-m}. \quad (29)$$

Proof. By plugging (1) and (26) in (28), and with the help of [15, 7.522 Eq. (9) and 9.121 Eq. (1)] one can obtain (29). ■

Proposition 6. *The ABEP for DQPSK scheme with Gray coding over the $\kappa - \mu$ shadowed fading channel can be tightly approximated as*

$$P_e \simeq \frac{\lambda\eta}{\Gamma(\mu)} \sum_{i=0}^2 \left[\mathcal{C}_i \mathcal{M}_{i,k}^{(1)}(a) - \mathcal{C}_i \mathcal{M}_{i,k}^{(1)}(-a) + \frac{\mathcal{F}_i}{\eta} \mathcal{M}_{i,k}^{(2)} \right], \quad (30)$$

with

$$\mathcal{M}_{i,k}^{(1)}(a) = \sum_{k=0}^{\infty} \frac{\phi_{i,k} {}_2F_1\left(\frac{1}{2}, \mu + k; \mu + k + 1; \frac{2\xi_i}{(b-a)^2 + 2\xi_i}\right)}{2\sqrt{\pi}}, \quad (31)$$

$$\mathcal{M}_{i,k}^{(2)} = \sum_{k=0}^{\infty} \psi_{i,k} {}_2F_1\left(\frac{\mu + k}{2}, \frac{\mu + k + 1}{2}; 1; \frac{2}{(2 + \xi_i)^2}\right), \quad (32)$$

$$\phi_{i,k} = \frac{(m)_k \omega^k}{(\mu)_k k!} \left(\frac{2}{(b-a)^2 + 2\xi_i} \right)^{\mu+k} \frac{\Gamma(\mu + k + \frac{1}{2})}{\mu + k}, \quad (33)$$

$$\psi_{i,k} = \frac{\Gamma(\mu) (m)_k \omega^k}{k! (2 + \xi_i)^{\mu+k}}, \quad (34)$$

$$\xi_i = \nu + \mathcal{D}_i, \quad (35)$$

$$\eta = \frac{1 - \delta^2}{\delta}, \quad (36)$$

where (\cdot) represents the pochhammer symbol, ${}_2F_1(\cdot, \cdot; \cdot; \cdot)$ denotes the hypergeometric functions [15, Eq. (8.310)], $\mathcal{F}_0 = \mathcal{C}_0$, $\mathcal{F}_1 = \mathcal{C}_1$, $\mathcal{F}_2 = -\frac{1}{2}$, $\mathcal{F}_2 = \frac{\delta^2}{1-\delta^2}$, and $\mathcal{D}_2 = 0$.

Proof. First, one can check using (9) and (17) jointly with (10), (21), and (22)

$$\tilde{\mathcal{H}}_0(\gamma) = \eta \sum_{i=0}^2 \left[\mathcal{C}_i e^{-\mathcal{D}_i \gamma} \mathcal{K}(a, b, \gamma) + \mathcal{F}_i e^{-(2+\mathcal{D}_i)\gamma} I_0(\sqrt{2}\gamma) \right]. \quad (37)$$

On the other hand, the ABEP for DQPSK can be evaluated as

$$P_s = \int_0^{\infty} f(\gamma) \mathcal{H}_2(\gamma) d\gamma. \quad (38)$$

Now, using (26) and (37) in (38), the ABEP can be approximated by

$$P_e \simeq \frac{\lambda\eta}{\Gamma(\mu)} \sum_{i=0}^2 \left[\mathcal{C}_i \mathcal{M}_{i,k}^{(1)}(a) - \mathcal{C}_i \mathcal{M}_{i,k}^{(1)}(-a) + \frac{\mathcal{F}_i}{\eta} \mathcal{M}_{i,k}^{(2)} \right] \quad (39)$$

where

$$\begin{aligned} \mathcal{M}_i^{(1)}(a) &= \int_0^{\infty} \gamma^{\mu-1} {}_1F_1(m; \mu; \omega\gamma) e^{-(\mathcal{D}_i + \nu)\gamma} \\ &\quad \times Q((b-a)\sqrt{\gamma}) d\gamma, \end{aligned} \quad (40)$$

and

$$\mathcal{M}_i^{(2)} = \int_0^\infty \gamma^{\mu-1} {}_1F_1(m; \mu; \omega\gamma) e^{-(2+\xi_i)\gamma} I_0(\sqrt{2}\gamma) d\gamma. \quad (41)$$

Utilizing Craig's formula of the Gaussian Q -function [34, Eq. (5)] and [15, 9.14.1], (40) can be written as

$$\begin{aligned} \mathcal{M}_i^{(1)}(a) &= \sum_{k=0}^{\infty} \frac{(m)_k}{(\mu)_k} \frac{\omega^k}{k!} \frac{1}{\pi} \int_0^{\frac{\pi}{2}} \int_0^\infty \gamma^{\mu+k-1} \\ &\quad \times \exp\left(-\left(\frac{(b-a)^2}{2\sin^2(\theta)} + \xi_i\right)\gamma\right) d\gamma d\theta \end{aligned} \quad (42)$$

By evaluating the inner integral in (42) with the aid of [15, Eq. (3.381.4)], we get

$$\begin{aligned} \mathcal{M}_i^{(1)}(a) &= \sum_{k=0}^{\infty} \frac{(m)_k \omega^k \Gamma(\mu+k) \int_0^{\frac{\pi}{2}} \left(\frac{(b-a)^2}{2\sin^2(\theta)} + 2\xi_i\right)^{-\mu-k} d\theta}{\pi (\mu)_k k!} \\ &= \sum_{k=0}^{\infty} \frac{(m)_k \omega^k \Gamma(\mu+k) 2^{\mu+k}}{\pi (\mu)_k k!} \\ &\quad \times \int_0^{\frac{\pi}{2}} \left(\frac{\sin^2(\theta)}{(b-a)^2 + 2\xi_i - 2\xi_i \cos^2(\theta)}\right)^{\mu+k} d\theta \end{aligned} \quad (43)$$

Now, by substituting [15, Eq. (3.682)] into (43), (31) is obtained. Finally, (41) can be evaluated relying on [15, Eqs. (9.14.1) and (6.621.1)] to obtain (32), which concludes the proof. ■

A. Asymptotic Analysis

In order to gain further insights into system parameters at high SNR regime, an asymptotic analysis for the SNR is carried out. Firstly, note that for large values of $\bar{\gamma}$, one can see that ω goes to 0 and thus the term $k = 0$ dominates the others, v also goes to 0 (i.e., $\xi_i \simeq \mathcal{D}_i$). It follows that the AEP can be asymptotically approximated as

$$P_e \sim \lambda \sum_{l=1}^7 \mathcal{A}_l \mathcal{B}_l^{-\mu}. \quad (44)$$

and

$$P_e \sim \frac{\lambda\eta}{\Gamma(\mu)} \sum_{i=0}^2 \left[\mathcal{C}_i \mathcal{M}_i^{(1,asy)}(a) - \mathcal{C}_i \mathcal{M}_i^{(1,asy)}(-a) + \frac{\mathcal{F}_i}{\eta} \mathcal{M}_i^{(2,asy)} \right], \quad (45)$$

for M -PSK and DQPSK schemes, respectively, with

$$\mathcal{M}_i^{(1,asy)}(a) \sim \Delta {}_2F_1\left(\frac{1}{2}, \mu; \mu + 1; \frac{2\mathcal{D}_i}{(b-a)^2 + 2\mathcal{D}_i}\right), \quad (46)$$

$$\Delta = \frac{1}{2\sqrt{\pi}} \left(\frac{2}{(b-a)^2 + 2\mathcal{D}_i}\right)^\mu \frac{\Gamma(\mu + \frac{1}{2})}{\mu}, \quad (47)$$

$$\mathcal{M}_i^{(2,asy)} \sim \frac{\Gamma(\mu)}{(2 + \mathcal{D}_i)^\mu} {}_2F_1\left(\frac{\mu}{2}, \frac{\mu + 1}{2}; 1; \frac{2}{(2 + \mathcal{D}_i)^2}\right). \quad (48)$$

It is worth mentioning from (44) and (45) alongside with (27) that the diversity order equals μ .

B. Bound on the truncation error

The above approximate ABEP for DQPSK is expressed in terms of infinite series. Truncating such summation and estimating the truncated error is though of paramount importance for numerical evaluation purposes. In what follows, a closed-form bound for such truncation error is provided.

Using (31), the truncation up to $L - 1$ terms of the first summation results to the following error

$$\epsilon_i^{(1)}(a) = \sum_{k=L}^{\infty} \frac{\phi_k}{2\sqrt{\pi}} {}_2F_1\left(\frac{1}{2}, \mu + k; \mu + k + 1; \frac{2\xi_i}{(b-a)^2 + 2\xi_i}\right) \quad (49)$$

By changing the summation index to $j = k - L$ in (49), then using [35, Eq. (06.10.02.0001.01)], and performing some manipulations, the bound can be expressed as

$$\begin{aligned} \epsilon_i^{(1)}(a) &\leq \frac{\Theta_{i,L}(a)}{2\sqrt{\pi}} {}_1F_0\left(\frac{1}{2}; -; \frac{2\xi_i}{(b-a)^2 + 2\xi_i}\right) \\ &\quad \times {}_2F_1\left(1, m + L; L + 1; \frac{2\omega}{(b-a)^2 + 2\xi_i}\right), \end{aligned} \quad (50)$$

with

$$\begin{aligned} \Theta_{i,L}(a) &= \left(\frac{2}{(b-a)^2 + 2\xi_i}\right)^\mu \frac{\Gamma(\mu) \Gamma(m + L)}{L! \Gamma(m)} \\ &\quad \times \left(\frac{2\omega}{(b-a)^2 + 2\xi_i}\right)^L. \end{aligned} \quad (51)$$

In a similar manner, the truncated error of the summation (32) can be upper bounded by

$$\begin{aligned} \epsilon_i^{(2)} &\leq \Lambda_{i,L} {}_2F_1\left(\frac{\mu + L}{2}, \frac{\mu + L + 1}{2}; 1; \frac{2}{(2 + \xi_i)^2}\right) \\ &\quad \times {}_2F_1\left(1, m + L; L + 1; \frac{\omega}{2 + \xi_i}\right), \end{aligned} \quad (52)$$

with

$$\Lambda_{i,L} = \frac{\Gamma(\mu) \omega^L}{L! \Gamma(m+L) \Gamma(m) (2 + \xi_i)^{\mu+L}}. \quad (53)$$

Consequently, and having in mind that $\epsilon_i^{(j)}$ are positives, as can be seen from 50 and 52, the absolute value of the total truncated error can be upper bounded by

$$|\epsilon_{P_b}| \leq \frac{\lambda \eta}{\Gamma(\mu)} \sum_{i=0}^2 \left[\mathcal{C}_i \epsilon_i^{(1)}(a) + \mathcal{C}_i \epsilon_i^{(1)}(-a) + \frac{\mathcal{F}_i \epsilon_i^{(2)}}{\eta} \right]. \quad (54)$$

V. RESULTS AND DISCUSSION

In this section, the proposed approximation for the AEP versus SNR (in dB) for both M -PSK and DQPSK modulation schemes over $\kappa - \mu$ shadowed fading channel is evaluated and compared with the exact one for various fading severity parameters.

- Figs. 3 and 7 illustrate, for a fixed value of m , the effect of parameter μ on the AEP for M -PSK and DQPSK modulation techniques, respectively under a weak line of sight (LOS) condition. One can notice that the greater the μ is, the better the system's performance.
- Figs. 4 and 8 depict the AEP for both considered modulation schemes under strong LOS ($\kappa = 10$) for a fixed value of μ . It is observed that countering the effect of shadowing requires the increase of m .
- To show the versatility of the $\kappa - \mu$ shadowed fading, Figs. 5, 6, and 9 present the AEP for some classical fading models. Noteworthy, the results in all figures are provided for either integer or non-integer values of μ and m . Further, the simulation curves match perfectly with the proposed approximation.
- Fig. 10 depicts the absolute value of the truncated error versus the number of limited terms L for DQPSK modulation. It can be shown that the greater L is, the smaller such an error. Interestingly, the truncated error decreases with the increase of SNR.
- Lastly, Fig. 11 presents the achievable diversity order for both modulation schemes versus the average SNR, computed by evaluating $-\frac{\log P_s}{\log \bar{\gamma}}$. It is clearly noticed that such a metric goes to μ as $\bar{\gamma}$ tends to infinity.

VI. CONCLUSION

New approximate expressions for the EP of a communication system employing either M -PSK or DQPSK modulation have been derived. The proposed approximations ensures optimal accuracy-analytical tractability trade-off that enables its versatility to contribute to the AEP

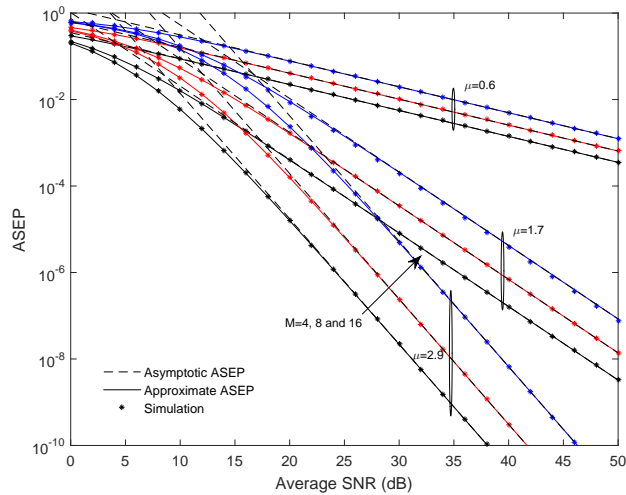


Fig. 3. ASEP for M -PSK under weak LOS scenario ($\kappa = 1$) with different values of μ and $m = 1.3$.

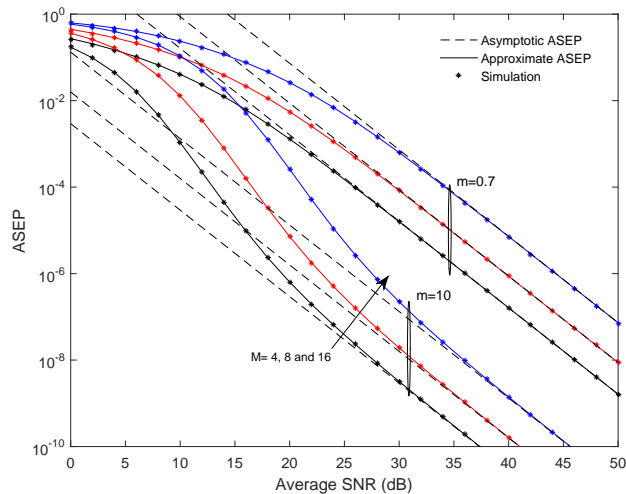


Fig. 4. ASEP for M -PSK under strong LOS scenario ($\kappa = 10$) with different values of m and $\mu = 2$.

computation over generalized fading channel. The resulting accuracy is better than that reached by other existing works relying on more complex mathematical expressions. Furthermore, a new closed-form approximation for the AEP under $\kappa - \mu$ shadowed fading model has been investigated and it is accurate for all the practical values of the SNRs, and are valid for the entire range of the shaping parameters κ , μ , and m . As far as we know, no previous works dealt

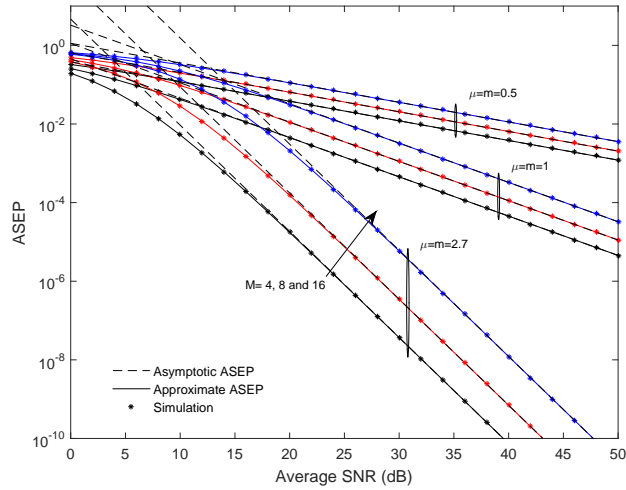


Fig. 5. ASEP for M -PSK under non-LOS scenario ($\kappa = 0$) with $\mu = m$.

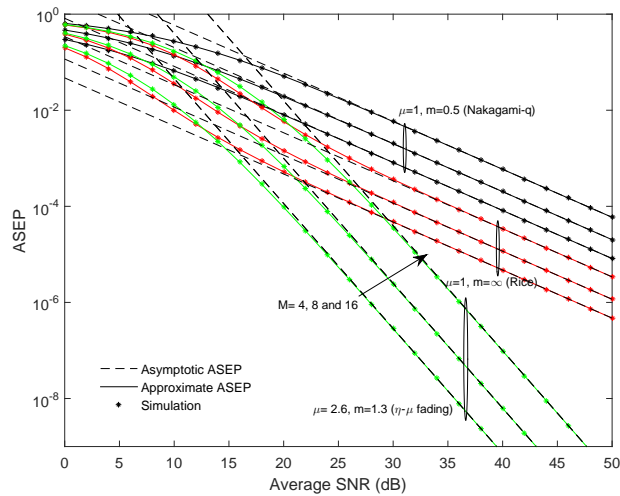


Fig. 6. ASEP for M -PSK over various practical fading models with $\kappa = 5$.

with such fading and modulation scheme with such a simple approximation. As a future aspect, the authors aim to extend the same approach on more general fading model such as $\alpha - \kappa - \mu$ shadowed [36] and fluctuating Beckmann fading models [37].

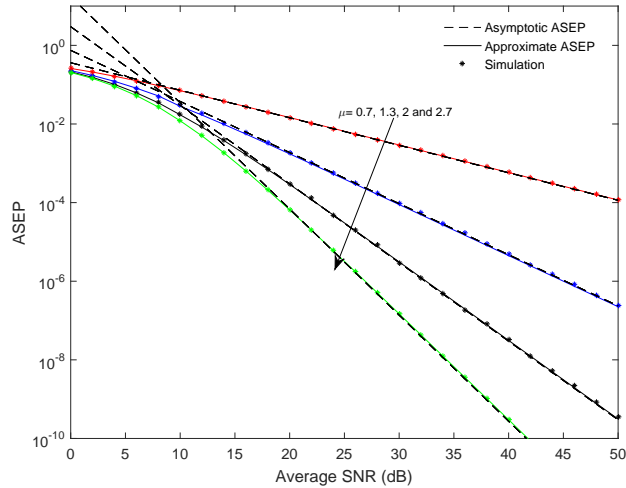


Fig. 7. ABEP for DQPSK under weak LOS scenario ($\kappa = 1$) with different values of μ and $m = 1.3$.

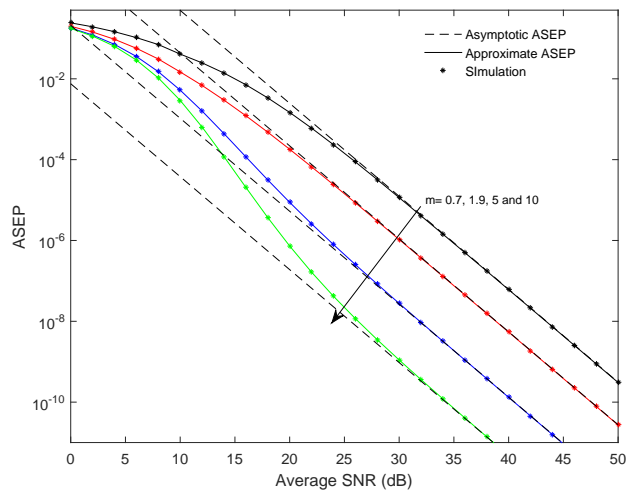


Fig. 8. ABEP for DQPSK under strong LOS scenario ($\kappa = 10$) with different values of m and $\mu = 2.3$.

ABBREVIATIONS

AEP: average error probability; ABEP: average bit error probability; ASEP: average symbol error probability; AWGN: additive white Gaussian noise; DQPSK: differential quaternary phase-shift keying; EP: error probability; LOS: line of sight; MQF: Marcum Q -function of the first order; MBF: modified Bessel function; PDF: probability density function; PSK: phase-shift keying

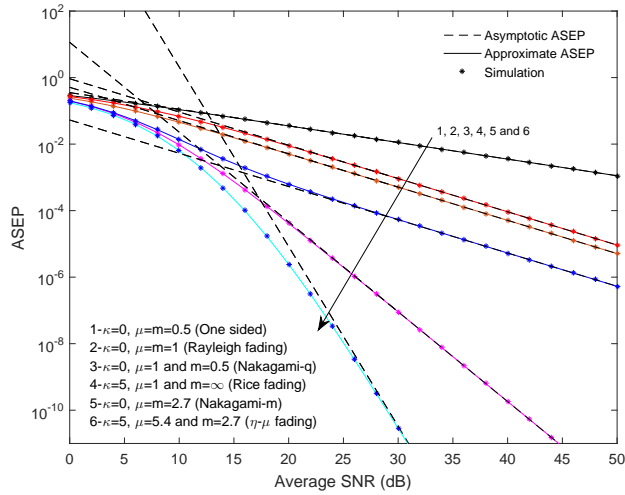


Fig. 9. ABEP for DQPSK over numerous practical fading distributions with $\kappa = 5$.

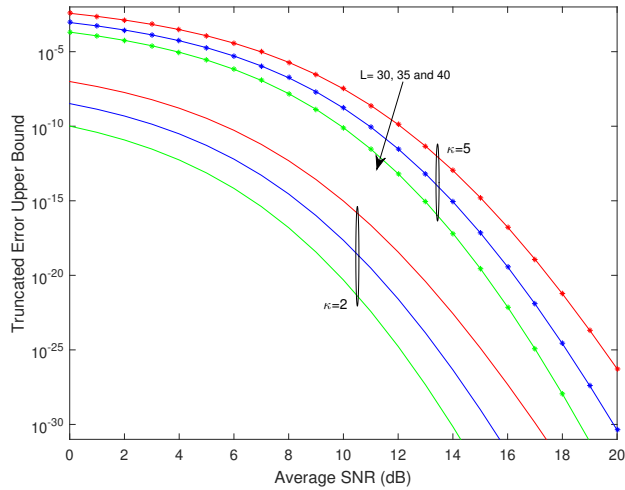


Fig. 10. Upper bound for the truncated error for $\mu = 2.3$ and $m = 4.7$ and various values of κ and L .

modulation schemes; SEP: symbol error probability; SNR: signal-to-noise ratio; UIFH: upper incomplete upper Fox’s H-function.

DECLARATIONS

Ethics Approval and Consent to Participate

The authors declare that this subsection is not applied for this work.

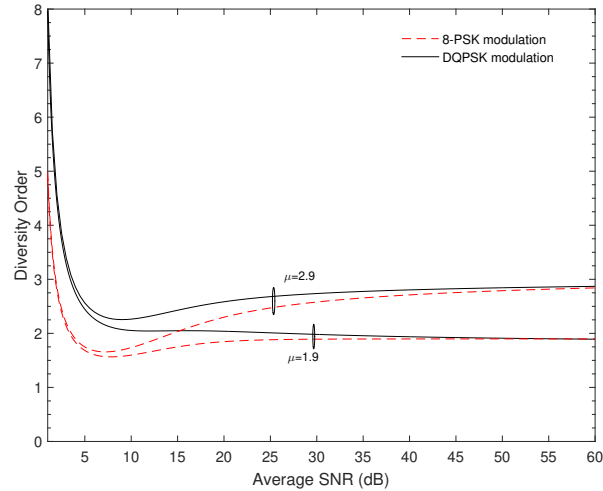


Fig. 11. Diversity order for $\kappa = 5$, $m = 4.7$ and various values of μ under M -PSK and DQPSK modulation schemes.

Consent for Publication

The authors declare that they wrote completely all scripts associated with the results presented in this work (i.e., figures and tables). No script or data has been imported or used from subsection is not applied for this work.

Availability of Data and Material

All scripts related to this work, developed by the two authors, can be found in github.com/FaissalEIBouanani/M

Competing interests

The authors declare that they have no competing interests.

Funding

The authors received no specific funding for this work.

Authors' contributions

YM derived new approximate expressions for (i) Marcum Q -function of the first order and (ii) SEP integral-form for M -PSK modulation. Based on these two results, YM and FE derived the approximate expressions for ASEP under both modulation schemes along with their asymptotic

form and the achievable diversity order. YM performed the simulations. YM and FE wrote the paper, analyze and revise the results. All authors read and approved the final manuscript.

Acknowledgment

The paper has been developed and written exclusively by the two authors.

REFERENCES

- [1] M. K. Simon and M.-S. Alouini, *Digital communications over fading channels*, 2nd edition, John Wiley & Sons, 2005.
- [2] M. D. Yacoub, "The $\alpha - \mu$ distribution: A physical fading model for the Stacy distribution," *IEEE Trans. Veh. Technol.*, vol. 56, no. 1, pp. 27–34, Jan. 2007.
- [3] M. D. Yacoub, "The $\eta - \mu$ distribution and the $\kappa - \mu$ distribution," *IEEE Antennas Propag. Mag.*, vol. 49, no. 1, pp. 68–81, Feb. 2007.
- [4] G. Fraidenraich and M. D. Yacoub, "The $\alpha - \eta - \mu$ and $\alpha - \kappa - \mu$ fading distributions," 2006, pp. 16–20, Manaus, Amazon, Brazil.
- [5] R. Cogliatti and R. A. A. de Souza, "A near-100% efficient algorithm for generating $\alpha - \kappa - \mu$ and $\alpha - \eta - \mu$ variates," 2013, pp. 1–5, Las Vegas, NV, USA.
- [6] J. F. Paris, "Statistical characterization of $\kappa - \mu$ shadowed fading," *IEEE Trans. Veh. Technol.*, vol. 63, no. 2, pp. 518–526, Feb. 2014.
- [7] S. L. Cotton, "Human body shadowing in cellular device to device communications: Channel modeling using the shadowed $\kappa - \mu$ fading model," *IEEE J. Sel. Areas Commun.*, vol. 33, no. 1, pp. 111–119, Jan. 2015.
- [8] "Shadowed fading in body-to-body communications channels in an outdoor environment at 2.45 GHz," in *Proc. IEEE-APS Topical Conf. Antennas Propag. Wireless Commun. (APWC)*, Palm Beach, FL, USA, Aug. 2014, pp. 249–252.
- [9] F. J. Canete, J. Lopez-Fernandez, C. Garcia-Corrales, A. Sanchez, E. Robles, F. J. Rodrigo, and J. F. Paris, "Measurement and modeling of narrowband channels for ultrasonic underwater communications," *Sensors*, vol. 16, no. 2, Feb. 2016.
- [10] Y. J. Chun, S. L. Cotton, H. S. Dhillon, F. J. Lopez-Martinez, J. F. Paris and S. K. Yoo, "A comprehensive analysis of 5G heterogeneous cellular systems operating over $\kappa - \mu$ shadowed fading channels," *IEEE Trans. Wireless Commun.*, vol. 16, no. 11, pp. 6995–7010, Nov. 2017.
- [11] J. Zhang, X. Li, I. S. Ansari, Y. Liu, and K. A. Qaraqe, "Performance analysis of dual-hop satellite relaying over $\kappa - \mu$ shadowed fading channels," in *Proc. IEEE Wireless Commun. Networking Conf. (WCNC)*, San Francisco, CA, USA, Mar. 2017, doi: 10.1109/WCNC.2017.7925541.
- [12] L. Moreno-Pozas, F. J. Lopez-Martinez, J. F. Paris and E. Martos- Naya, "The $\kappa - \mu$ shadowed fading model: Unifying the $\kappa - \mu$ and $\eta - \mu$ distributions," *IEEE Trans. Veh. Technol.*, vol. 65, no. 12, pp. 9630–9641, Dec 2016.
- [13] F. J. Lopez-Martinez, J. F. Paris and J. M. Romero-Jerez, "The $\kappa - \mu$ shadowed fading model with integer fading parameters." *IEEE Trans. Veh. Technol.* vol. 66, no. 9, pp. 7653–7662, Sep. 2017.
- [14] J.G. Proakis, *Digital Communications*, 4th edition, New-York: McGraw-Hill, 2001.
- [15] A. Jeffrey and D. Zwillinger, *Table of integrals, series, and products*. Elsevier, 2007.
- [16] C. Chie, "Bounds and approximations for rapid evaluation of coherent MPSK error probabilities," *IEEE Trans. Commun.*, vol. 33, no. 3, pp. 271–273, Mar. 1985.
- [17] J. J. Komo and K. D. Barnett, "Improved bounds for coherent M-ary PSK symbol error probability," *IEEE Trans. Veh. Technol.*, vol. 46, no. 2, pp. 396–399, May. 1997.

- [18] S. Park, D. Yoon and K. Cho, "Tight approximation for coherent MPSK symbol error probability," *Electron. Lett.*, vol. 39, no. 16, pp. 1220–1222, 7 Aug. 2003.
- [19] L. Rugini "SEP Bounds for MPSK with Low SNR," in *IEEE Commun. Lett.*, doi: 10.1109/LCOMM.2020.3012837..
- [20] F. El Bouanani, Y. Mouchtak and G. K. Karagiannidis, "New Tight Bounds for the Gaussian Q-Function and Applications," in *IEEE Access*, doi: 10.1109/ACCESS.2020.3015344.
- [21] Y. Mouchtak, F. El Bouanani, and D. B. da Costa, "Tight analytical and asymptotic upper bound for the BER and FER of linear codes over exponentially correlated generalized-fading channels," *IEEE Trans. Commun.*, vol. 67, no. 6, pp. 3852-3864, June 2019.
- [22] P. Y. Kam and R. Li., "Computing and bounding the first-order Marcum Q-fuction: A geometric approach," *IEEE Trans. Comms.*, vol. 56, no. 7, pp. 1101-1110, July 2008.
- [23] P. Y. Kam and R. Li, "Simple tight exponential bounds on the first-order Marcum Q -function via the geometric approach," *2006 IEEE Int. Sym. Trans. Info. Theory*, Seattle, WA, 2006, pp. 1085-1089.
- [24] J. Wang and D. Wu, "Tight bounds for the Marcum Q -function," *Wirel. Commun. Mob. Comput.*, 2010.
- [25] G. D. Zhao, X and Y. Li, "Tight geometric bound for marcum qfunction," *Electronics Letters*, vol. 44, no. 5, pp. 340-341, Feb 2008.
- [26] G. Ferrari and G.E. Corazza, "Tight bounds and accurate approximations for DQPSK transmission bit error rate," *Electronics Letters*, vol. 40, no. 20, pp. 1284-1285, Sep. 2004.
- [27] Y. Sun, A. Baricz, M. Zhao, X. Xu, and S. Zhou, "Approximate average bit error probability for DQPSK over fading channels," *Electronics Letters*, vol. 45, no. 23, pp. 1177-1179, Nov. 2009.
- [28] A. Baricz, A. Szilárd, and J. Fodor, "New approximations for DQPSK transmission bit error rate," *IEEE 8th International Symposium on Applied Computational Intelligence and Informatics (SACI)*, May. 2013, pp. 73-77.
- [29] J. Abouei, K. N. Plataniotis, and S. Pasupathy, "Green modulations in energy-constrained wireless sensor networks," *IET Communications*, vol. 5, no. 2, pp. 240-251, 2011.
- [30] B. Natarajan, C. R. Nassar, and S. Shattil, "CI/FSK: bandwidth-efficient multicarrier FSK for high performance, high throughput, and enhanced applicability," *IEEE Trans. Commun.*, vol. 52, no. 3, pp. 362-367, Mar. 2004.
- [31] F. F. Digham, M.-S. Alouini, and S. Arora, "Variable-rate variable-power non-coherent M-FSK scheme for power limited systems," *IEEE Trans. Wirel. Commun.*, vol. 5, no. 6, pp. 1306-1312, June 2006.
- [32] Sadhwani, Dharmendra, Ram Narayan Yadav, and Supriya Aggarwal, "Tighter Bounds on the Gaussian Q -Function and Its Application in Nakagami- m Fading Channel," *IEEE Wirel. Communic. Lett.*, vol. 6, no. 5, pp. 574-577, June 2017.
- [33] J. A. Cochran, "The monotonicity of modified Bessel functions with respect to their order", *Journal of Mathematics and Physics*, vol. 46, no 1-4, pp. 220-222, 1967.
- [34] J. W. Craig, "A New, Simple and Exact Result for Calculating the Probability of Error for Two-Dimensional Signal Constellations," in *Proc. of the IEEE Military Commun. Conf., McLean, USA*, Nov. 1991, pp. 571-575.
- [35] I. W. Research, Mathematica Edition: version 12.1 Campaign, Illinois: Wolfram Research, Inc., 2020.
- [36] P. Ramirez-Espinosa, et al. "The $\alpha - \kappa - \mu$ Shadowed Fading Distribution: Statistical Characterization and Applications," in *2019 IEEE Global Communications Conference (GLOBECOM)*, Waikoloa, HI, USA, 2019, doi: 10.1109/GLOBECOM38437.2019.9013399.
- [37] P. Ramirez-Espinosa, F. J. Lopez-Martinez, J. F. Paris, M. D. Yacoub, and E. Martos-Naya, "An extension of the $\kappa - \mu$ shadowed fading model: Statistical characterization and applications," *IEEE Trans. Veh. Technol.*, vol. 67, no. 5, pp. 3826-3837, May 2018.

FIGURE LEGENDS

- Fig. 1 Comparison between $\chi(\gamma)$ and $\tilde{\chi}(\gamma)$. To show the accuracy of the fitting method, Fig. 1 depicts the curves of both exact and approximated fitting coefficients.
- Fig. 2 Comparison of the relative errors. To demonstrate the tightness of the proposed EP's approximate expressions for GC-DQPSK modulation, Fig. 2 depicts the absolute relative error of the proposed approximation with solid line as well as the best ones proposed in the literature.
- Fig. 3 ASEP for M -PSK under weak LOS scenario ($\kappa = 1$) with different values of μ and $m = 1.3$. The approximated ASEP is presented with solid line, the simulated one with marker and dashed line presents the asymptotic ASEP.
- Fig. 4 ASEP for M-PSK under strong LOS scenario ($\kappa = 10$) with different values of m and $\mu = 2$. The approximated ASEP is presented with solid line, the simulated one with marker and dashed line presents the asymptotic ASEP.
- Fig. 5 ASEP for M-PSK under non-LOS scenario ($\kappa = 0$) with $\mu = m$. The approximated ASEP is presented with solid line, the simulated one with marker and dashed line presents the asymptotic ASEP.
- Fig. 6 ASEP for M-PSK over various practical fading models with ($\kappa = 5$). The approximated ASEP is presented with solid line, the simulated one with marker and dashed line presents the asymptotic ASEP.
- Fig. 7 ABEP for DQPSK under weak LOS scenario ($\kappa = 1$) with different values of μ and $m = 1.3$. The approximated ABEP is presented with solid line, the simulated one with marker and dashed line presents the asymptotic ABEP.
- Fig. 8 ABEP for DQPSK under strong LOS scenario ($\kappa = 10$) with different values of m and $\mu = 2.3$. The approximated ABEP is presented with solid line, the simulated one with marker and dashed line presents the asymptotic ABEP.
- Fig. 9 ABEP for DQPSK over numerous practical fading distributions with ($\kappa = 5$). The approximated ABEP is presented with solid line, the simulated one with marker and dashed line presents the asymptotic ABEP.
- Fig. 10 Upper bound for the truncated error for $\mu = 2.3$ and $m = 4.7$ and various values of (κ) and L .
- Fig. 11 Diversity order for $\kappa = 5$, $m = 4.7$ and various values of μ under M-PSK and

DQPSK modulation schemes. The diversity curve of M -PSK modulation is presented by dashed line while the solid line presents that for GC-DQPSK modulation.